

Performance of 3-D Infinite Elements for High-Frequency Electromagnetic Fields

Yuta Watanabe, Yuki Sato, and Hajime Igarashi

Graduate School of Information Science and Technology, Hokkaido University, Kita-ku Sapporo 060-0814, Japan

The infinite elements for edge based finite-element methods (FEMs) have been shown effective for open boundary problems. In the infinite elements, electromagnetic fields are expressed in terms of radially decaying basis functions. On the other hand, the perfect matched layer has widely been used for FEMs for high-frequency problems. In this paper, numerical performance of both methods is comparably discussed. The numerical experiments show that the former has higher computational efficiency.

Index Terms—Finite-element method (FEM), high-frequency problem, infinite element, perfect matched layer (PML).

I. INTRODUCTION

HIGH-FREQUENCY electromagnetic field computations using the finite-difference time-domain (FDTD) method, finite-element method (FEM), and method of moment (MoM) have widely been performed [1], [2]. The MoM has an advantage to deal with the infinite region without introducing artificial open boundaries. However we must solve equations including a dense matrix for MoM analysis. The FDTD method can effectively solve large scale problems because it is an explicit method. If analysis model includes curved surfaces or structures whose scale is much smaller than the whole scale, the FDTD method needs a great number of unknowns because it employs cuboid cells.

FEM can effectively analyze electromagnetic fields in complicated geometries because it can employ the tetrahedron or hexahedron elements. To solve high-frequency electromagnetic field problems using FEM, the infinite elements [3]–[6] and perfectly matched layer (PML) [7], [8] have been employed to treat open boundaries. The infinite element has been shown effective for static, quasi-static [9] and high-frequency electromagnetic field analysis [10], [11]. The infinite elements have been discussed for sound and electromagnetic waves in [4] and [5], respectively. Although the formulation in [5] is mathematically rigorous, the resultant finite element (FE) matrix is asymmetric. Although the formulation in [4] is valid only for spherical domains, the FE matrix is symmetric. In this study, we consider the symmetric formulations of the infinite elements presented in [4], which has been extended to electromagnetic waves in [6]. In the infinite elements, electromagnetic fields are expressed in terms of radially decaying basis functions. It has been shown that the infinite element method results in ill-conditioned FE matrices. This problem must be overcome to apply the infinite elements to large scale problems. Moreover the performance of the infinite elements for high-frequency problems has not been compared with that of PML.

In this study, the matrix conditioning for the infinite elements applied to high-frequency problems is improved by orthogonalization of the basis functions, which has been shown effective for static fields [9]. The numerical performance of the 3-D infinite elements and PML is comparatively discussed.

This paper will be organized as follows: in Section II, FEM using the infinite element will be formulated. In Section III, numerical results will be presented which show effectiveness of the infinite element.

II. FORMULATION

A. Governing Equation

The weak form for high-frequency electromagnetic fields is given by

$$\int_{\Omega} [(\nu \nabla \times \mathbf{A}) \cdot (\nabla \times \mathbf{W}) - \omega^2 \epsilon \mathbf{A} \cdot \mathbf{W}] dv + \int_{\partial\Omega} \mathbf{W} \times \mathbf{H} \cdot \mathbf{n} ds = \int_{\Omega} \mathbf{J} \cdot \mathbf{W} dv \quad (1)$$

where \mathbf{A} , \mathbf{W} , \mathbf{H} and \mathbf{J} denote the vector potential, weighting vector magnetic field and current density, respectively. Moreover, ν , ω and ϵ denote the inverse of permeability, driving frequency and complex permittivity. In this study, (1) is solved by FEM in which the finite domain is discretized with hexahedral elements while open boundaries are treated by the infinite elements.

B. Formulation of Infinite Element [6]

Fig. 1 illustrates the infinite element in which unknowns are assigned to the eight edges. The infinite element is formed by linearly extending the outermost boundary of the finite region from the reference point $\mathbf{X}_0(x_0, y_0, z_0)$ to the infinite point. The position vector \mathbf{x} in the infinite element can be expressed as

$$\mathbf{x} = \mathbf{X}_0 + t \left(\sum_{i=1}^4 \omega_i(r, s) \mathbf{x}_i - \mathbf{X}_0 \right) \quad (1)$$

where \mathbf{x}_i is the position vector of the i th node on the outermost boundary and $\omega_i(r, s)$ is the interpolation function whose

Manuscript received November 10, 2012; revised December 28, 2012; accepted January 04, 2013. Date of current version May 07, 2013. Corresponding author: Y. Watanabe (e-mail: ywata@em-si.eng.hokudai.ac.jp).

Color versions of one or more of the figures in this paper are available online at <http://ieeexplore.ieee.org>.

Digital Object Identifier 10.1109/TMAG.2013.2240281

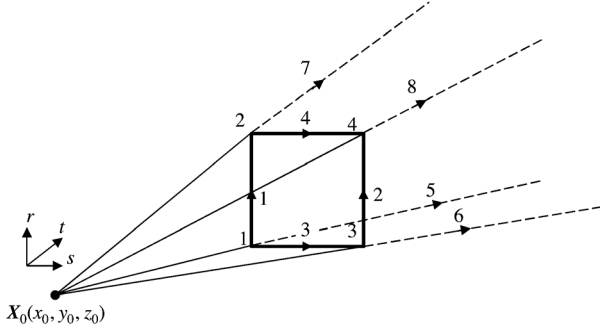


Fig. 1. Local coordinate of infinite element.

TABLE I
EXPLICIT FORMS OF $\omega_i(r, s)$

node number i	$\omega_i(r, s)$
1	$(1-r)(1-s)/4$
2	$(1+r)(1-s)/4$
3	$(1-r)(1+s)/4$
4	$(1+r)(1+s)/4$

explicit forms are summarized in Table I. The contravariant and covariant basis vector of the infinite element are given by

$$\mathbf{e}_r \equiv \frac{\partial \mathbf{x}}{\partial r} = t \sum_{i=1}^4 \frac{\partial \omega_i(r, s)}{\partial r} \mathbf{x}_i = t \mathbf{e}_{r1} \quad (2a)$$

$$\mathbf{e}_s \equiv \frac{\partial \mathbf{x}}{\partial s} = t \sum_{i=1}^4 \frac{\partial \omega_i(r, s)}{\partial s} \mathbf{x}_i = t \mathbf{e}_{s1} \quad (2b)$$

$$\mathbf{e}_t \equiv \frac{\partial \mathbf{x}}{\partial t} = \sum_{i=1}^4 \omega_i(r, s) \mathbf{x}_i = \mathbf{e}_{t1} \quad (2c)$$

$$\mathbf{e}^r \equiv \nabla r = \frac{\mathbf{e}_s \times \mathbf{e}_t}{\sqrt{g}} = \frac{\mathbf{e}_{s1} \times \mathbf{e}_{t1}}{t\sqrt{g_1}} = \frac{\mathbf{e}_1^r}{t} \quad (3a)$$

$$\mathbf{e}^s \equiv \nabla s = \frac{\mathbf{e}_t \times \mathbf{e}_r}{\sqrt{g}} = \frac{\mathbf{e}_{t1} \times \mathbf{e}_{r1}}{t\sqrt{g_1}} = \frac{\mathbf{e}_1^s}{t} \quad (3b)$$

$$\mathbf{e}^t \equiv \nabla t = \frac{\mathbf{e}_r \times \mathbf{e}_s}{\sqrt{g}} = \frac{\mathbf{e}_{r1} \times \mathbf{e}_{s1}}{t\sqrt{g_1}} = \frac{\mathbf{e}_1^t}{t} \quad (3c)$$

where \sqrt{g} is the Jacobian and the suffix "1" denotes the values on the quadrilateral $\{1, 2, 3, 4\}$ where $t = 1$. The metric tensors are defined by $g_{ij} = \mathbf{e}_i \cdot \mathbf{e}_j$ and $g^{ij} = \mathbf{e}^i \cdot \mathbf{e}^j$. It is assumed that the outermost boundary is a sphere whose center is at \mathbf{X}_0 so that the coordinates are orthogonal, i.e.,

$$g_{ij1} = \mathbf{e}_{i1} \cdot \mathbf{e}_{j1} = 0, \quad i \neq j. \quad (4)$$

The vector potential \mathbf{A} in the infinite element is approximated using the vector interpolation function \mathbf{N}_e^n as follows:

$$\mathbf{A} = \sum_{n=1}^N \sum_{e=1}^8 a_e^n \mathbf{N}_e^n \quad (5)$$

TABLE II
EXPLICIT FORMS OF (10) AND (11)

edge number e	$f_e(r, s)$	$g_e(r, s)$	edge number e	$\omega_e(r, s)$
1	$(1-s)/4$	0	5	$(1-r)(1-s)/4$
2	$(1+s)/4$	0	6	$(1+r)(1-s)/4$
3	0	$(1-r)/4$	7	$(1-r)(1+s)/4$
4	0	$(1+r)/4$	8	$(1+r)(1+s)/4$

where N is the expansion order of infinite element. The vector interpolation function \mathbf{N}_e^n is given by

$$\begin{aligned} \mathbf{N}_e^n &= \tau_n(t) e^{-jk\sqrt{g_{tt}}(t-1)} [f_e(r, s) \mathbf{e}^r + g_e(r, s) \mathbf{e}^s] \quad (1 < e < 4) \\ &= \frac{\tau_n(t)}{t} e^{-jk\sqrt{g_{tt}}(t-1)} [f_e(r, s) \mathbf{e}_1^r + g_e(r, s) \mathbf{e}_1^s] \quad (1 < e < 4) \\ &= \frac{\tau_n(t)}{t} e^{-jk\sqrt{g_{tt}}(t-1)} \mathbf{U}_e(r, s) \quad (1 < e < 4) \end{aligned} \quad (6)$$

$$\begin{aligned} \mathbf{N}_e^n &= \phi_n(t) e^{-jk\sqrt{g_{tt}}(t-1)} \omega_e(r, s) \mathbf{e}^t \quad (5 < e < 8) \\ &= \phi_n(t) e^{-jk\sqrt{g_{tt}}(t-1)} \mathbf{V}_e \quad (5 < e < 8) \end{aligned} \quad (7)$$

where k is the wavenumber and $g_{tt} = \mathbf{e}_t \cdot \mathbf{e}_t$ is approximately equal to the radius of the spherical domain. Equations (6) and (7) show in-plane and out-of-plane components of \mathbf{N}_e^n . The explicit forms of $f_e(r, s)$, $g_e(r, s)$ and $\omega_e(r, s)$ are shown in Table II. The functions τ_n and ϕ_n are defined by

$$\tau_n = \frac{1}{t^n}, \quad \phi_n = \frac{1}{t^{n+2}} \quad (n = 1, 2, \dots, N). \quad (8)$$

In this study, τ_0 and ϕ_0 are determined to approximate the far field radiation pattern of the high-frequency electromagnetic waves. The rotation of \mathbf{N}_e^n is given by

$$\begin{aligned} \nabla \times \mathbf{N}_e^n &= \frac{1}{t} \gamma_n e^{-jk\sqrt{g_{tt}}(t-1)} \mathbf{v}_e \\ &+ \frac{\tau_n}{t^2} e^{-jk\sqrt{g_{tt}}(t-1)} \mathbf{u}_e \quad (1 < e < 4) \end{aligned} \quad (9)$$

$$\nabla \times \mathbf{N}_e^n = \frac{\phi_n}{t} e^{-jk\sqrt{g_{tt}}(t-1)} \mathbf{w}_e \quad (5 < e < 8) \quad (10)$$

where

$$\mathbf{v}_e(r, s) = \frac{1}{\sqrt{g_1}} [-g_e(r) \mathbf{e}_{r1} + f_e(s) \mathbf{e}_{s1}], \quad (11a)$$

$$\mathbf{u}_e(r, s) = \frac{1}{\sqrt{g_1}} \left[\frac{dg_e(r)}{dr} - \frac{df_e(s)}{ds} \right] \mathbf{e}_{t1}, \quad (11b)$$

$$\mathbf{w}_e(r, s) = \frac{1}{\sqrt{g_1}} \left[\frac{\partial \omega_e(r, s)}{\partial s} \mathbf{e}_{r1} - \frac{\partial \omega_e(r, s)}{\partial r} \mathbf{e}_{s1} \right] \quad (11c)$$

$$\gamma_n(t) = \frac{\partial}{\partial t} \left(\tau_n e^{-jk\sqrt{g_{tt}}(t-1)} \right). \quad (11d)$$

When the weighting function \mathbf{W} in (1) is assumed to be the interpolation function \mathbf{N}_e^n , the local FE matrix corresponding to

the first term of L.H.S in (1) is given by

$$K_{e,e'}^{m,n} = (\mathbf{u}_e, \mathbf{u}_{e'}) \int_1^\infty \frac{\tau_m \tau_n}{t^2} e^{-j2k\sqrt{g_{tt}}(t-1)} dt + (\mathbf{v}_e, \mathbf{v}_{e'}) \int_1^\infty \gamma_m \gamma_n e^{-j2k\sqrt{g_{tt}}(t-1)} dt \quad (12a)$$

$$K_{e,e'}^{m,n} = (\mathbf{v}_e, \mathbf{w}_{e'}) \int_1^\infty \gamma_m \phi_n e^{-j2k\sqrt{g_{tt}}(t-1)} dt \quad (12b)$$

$$K_{e,e'}^{m,n} = (\mathbf{w}_e, \mathbf{w}_{e'}) \int_1^\infty \phi_m \phi_n e^{-j2k\sqrt{g_{tt}}(t-1)} dt \quad (12c)$$

Equations (12a), (12b), and (12c) include the inner products of two in-plane, in-plane and out-of-plane, and two out-of-plane components. In (12), the inner products among \mathbf{u}_e , \mathbf{v}_e and \mathbf{w}_e vanish due to the orthogonality (4) in the basis vectors. The local FE matrix corresponding to the second term of L.H.S in (1) is given by

$$M_{e,e'}^{m,n} = (\mathbf{U}_e, \mathbf{U}_{e'}) \int_1^\infty \tau_m \tau_n e^{-j2k\sqrt{g_{tt}}(t-1)} dt \quad (13a)$$

$$M_{e,e'}^{m,n} = (\mathbf{U}_e, \mathbf{V}_{e'}) \int_1^\infty t \tau_m \phi_n e^{-j2k\sqrt{g_{tt}}(t-1)} dt \quad (13b)$$

$$M_{e,e'}^{m,n} = (\mathbf{V}_e, \mathbf{V}_{e'}) \int_1^\infty t^2 \phi_m \phi_n e^{-j2k\sqrt{g_{tt}}(t-1)} dt. \quad (13c)$$

It is assumed that

$$\alpha_1 = \int_1^\infty e^{-j2k\sqrt{g_{tt}}(t-1)} dt = -e^{-j2k\sqrt{g_{tt}}} E_i(-j2k\sqrt{g_{tt}}) \quad (14a)$$

$$\alpha_l = \int_1^\infty \frac{e^{-j2k\sqrt{g_{tt}}(t-1)}}{t^l} dt = -\frac{1}{l-1} (-1 + 2jk\sqrt{g_{tt}} \alpha_{l-1}) \quad (14b)$$

where E_i is the exponential integral [12] and α_0 is the divergent integral. It can be found that the divergent integrals in (12a) and (13a) cancel out with the boundary term in (1).

C. Orthogonalization

In this study, we orthogonalize the first term in (11a) in order to improve the matrix conditioning. For simplicity, we express the integral in (12a) as

$$g_{n,m} = \int_1^\infty \frac{\tau_n \tau_m}{t^2} e^{-j2k\sqrt{g_{tt}}(t-1)} dt \quad (n, m = 0, 1, 2, \dots, N). \quad (15)$$

The gram matrix is given by

$$G = \begin{bmatrix} g_{0,0} & \cdots & g_{0,N} \\ \vdots & \ddots & \vdots \\ g_{N,0} & \cdots & g_{N,N} \end{bmatrix}. \quad (16)$$

The eigenvectors of G are arranged as column vectors in the matrix W . The gram matrix G is now orthogonalized as follows:

$$\hat{G} = W^t G W. \quad (17)$$

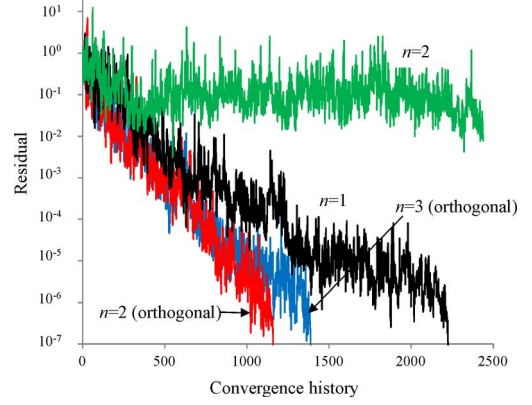


Fig. 2. Convergence history.

TABLE III
PERFORMANCE OF INFINITE ELEMENT AND PML

	iteration number	error (%)	CPU time
IE($n=2$)	1160	2.22	402.05
IE($n=3$)	1389	0.87	569.49
PML	2986	0.95	2249.1

III. NUMERICAL RESULTS

A. Loop Antenna

The electromagnetic fields around the rectangular loop antenna, 1 m per side, are computed by FEM using the infinite element and PML. The computational domain is a sphere whose radius is 2 m. The amplitude and frequency of driving current are 1 AT and 75 MHz, respectively. The thickness and conductivity of PML are set to 1 m and 0.00179 S/m so that the reflection from PML and iteration number of ICCG are minimized. Table III summarizes the iteration number of the ICCG method which solves the FE equation, errors in the magnetic field and CPU time of FEM using the infinite element and PML. The error is defined as follow:

$$\text{error} = \sqrt{\sum_i \left| \frac{B_i - B_{ai}}{B_{ai}} \right|^2} \quad (18)$$

where B_i and B_{ai} are magnetic flux densities obtained by the FEM and analytical solution in i th element. It is observed that the magnetic fields obtained by the present method and PML are in good agreement with the analytical solution. When the order of series expansion of the infinite element increases, the error decreases and iteration number increases. The results in Table III lead to the conclusion that the infinite element has higher computational efficiency in comparison with PML. Fig. 2 shows the residual histories of the ICCG method. It can be seen that the infinite element with $n = 2$ has poor convergence if the orthogonalization is not carried out.

B. Half-Wave Dipole Antenna

The electromagnetic fields around the half-wave dipole antenna are computed by FEM using the infinite element and PML. The parameters of the FEM are the same as those used in Section III-A. The electric field distributions obtained by

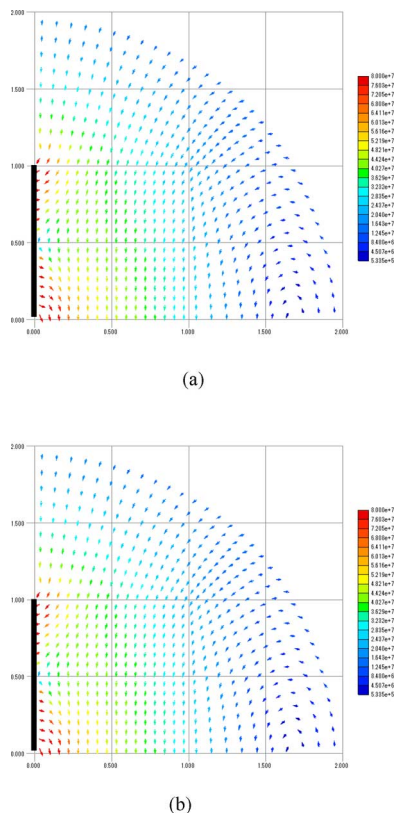


Fig. 3. Electric field computed by FEM using the infinite element in the finite region. (a) Infinite element (b) PML.

TABLE IV
PERFORMANCE OF INFINITE ELEMENT AND PML

	iteration number	CPU time
IE($n=2$)	2136	997.32
IE($n=3$)	2244	1147.23
PML	4646	5076.37

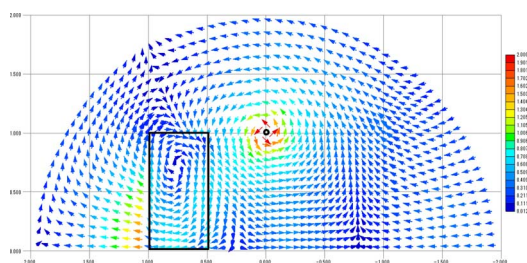


Fig. 4. Magnetic field computed by FEM using the infinite element with $n = 3$. The rectangle area is the cross section of the magnetic material.

FEM with the infinite element and PML are shown in Fig. 3. Both distributions seem almost identical. Table IV summarizes the iteration number of the ICCG method which solves the FE equation and CPU time of FEM using the infinite element and PML. The results in Table III lead to the conclusion that the infinite element has higher computational efficiency in comparison with PML.

C. Scattering Problem

The electromagnetic field around a brick-shaped magnetic material of $\mu_r = 10$, placed near the loop antenna mentioned in Section III-A, is computed using the present method. The driving frequency is set to 100 MHz. The FEM parameters are the same as those used in Section III-A. The resultant magnetic field distribution is shown in Fig. 4, which is found to be almost identical with that obtained by the FEM with PML.

IV. CONCLUSION

In this work, effectiveness of the infinite elements applied to wave problems has been discussed. The electromagnetic fields around the loop and half-wave dipole antennas are computed by FEM using the infinite element and PML. The results using the infinite element have good computational efficiency in comparison with PML. One of the drawbacks in the present method is that the domain boundary must be spherical. If the domain is not spherical, the formulation includes divergent integrals. In future work, we would resolve this problem.

ACKNOWLEDGMENT

The authors would like to thank Mr. A. Kameari of Science Solutions International Laboratory, Inc., who provided the invaluable comments on this study.

REFERENCES

- [1] A. Taflov, *Computational Electrodynamics, the Finite-Difference Time-Domain Method*. Norwood, MA, USA: Artech, 1998.
- [2] R. F. Harrington, *Field Computation by Moment Methods*. New York, NY, USA: Wiley-IEEE Press, 1993.
- [3] K. Gerdes, "A summary of infinite element formulations for exterior Helmholtz problems," *Comput. Methods Appl. Mech. Eng.*, vol. 164, no. 1–2, pp. 95–105, Oct. 1998.
- [4] D. S. Burnett, "A Three dimensional acoustic infinite element based on a prolate spheroidal multipole expansion," *J. Acoustic Soc. Am.*, vol. 96, pp. 2798–2816, 1994.
- [5] L. Demkowicz and M. Pal, "An infinite element for Maxwell's equations," *Computer Methods in Appl. Mechanics and Engineering*, vol. 164, pp. 77–94, 1998.
- [6] A. Kameari, "Electromagnetic analysis by finite element in frequency regime including displacement current (2)—Application of infinite element to open boundary problems," in *Proc. IEE Japan Papers Joint Tech. Meet. Static Apparatus Rotating Mach.*, 2011, pp. 73–78, SA-11, RM-11, in Japanese.
- [7] Z. S. Sacks, D. M. Kingsland, R. Lee, and J. F. Lee, "A perfectly matched anisotropic absorber for use as an absorbing boundary condition," *IEEE Transactions on Antennas and Propagation*, vol. 43, no. 12, pp. 1460–1463, 1995.
- [8] "An anisotropic perfectly match layer-absorbing medium for the truncation of FDTD lattices," *IEEE Trans. Antennas Propag.*, vol. 44, no. 12, pp. 1630–1639, Dec. 1996.
- [9] S. Tamitani, K. Tsuzaki, T. Tokumasu, Y. Takahashi, A. Kameari, H. Igarashi, K. Fujiwara, and Y. Ishihara, "Orthogonalized infinite edge element method—Convergence improvement by Orthogonalization of Hilbert matrix in infinite edge element method," *IEEE Trans. Magn.*, vol. 48, no. 2, pp. 363–366, Feb. 2012.
- [10] S. Gratkowski, L. Pichon, and A. Razek, "New infinite elements for a finite element analysis of 2-D scattering problems," *IEEE Trans. Magn.*, vol. 32, no. 3, pp. 882–885, Mar. 1996.
- [11] A. Charles, M. S. Towers, and A. Mccowen, "A general infinite element for terminating finite element meshes in electromagnetic scattering prediction," *IEEE Trans. Magn.*, vol. 34, no. 5, pp. 3367–3370, Sep. 1998.
- [12] M. Abramowitz and I. A. Stegun, *Handbook of Mathematical Functions With Formulas, Graphs, and Mathematical Tables*. New York, NY, USA: Dover, 1972.